

Supporting Information

Poly (acrylic acid) Locally Enriched in Slurry Enhances

Electrochemical Performance of the SiO_x Lithium-Ion Battery Anode

Ming Yang^{a,b}, Peng Chen^c, Jiapei Li^{b,d}, Ruoxuan Qi^{b,e}, Yudai Huang^d, Peter Müller-Buschbaum^{e,f}, Ya-Jun Cheng^{*b}, Kunkun Guo^{*c} and Yonggao Xia^{*b,g}

Content

Figure S1. Cycling performance of Li SiO _x cells at 0.5 C in the voltage range of 0.01 V - 1.5 V prepared with the slurries from water (PAA-H ₂ O) or DMF (PAA-DMF) with the mass loading density of SiO _x is 0.8 mg cm ⁻²	4
Figure S2. Cycling performance of Li SiO _x cells at 0.5 C in the voltage range of 0.01 V - 1.5 V prepared with the slurries from water (PAA-H ₂ O) or DMF (PAA-DMF) with the lithium metal counter electrode is replaced after more than 100 cycles.	5
Figure S3. Cycling performance of Li SiO _x cells at 0.5 C in the voltage range of 0.01 V - 1.5 V prepared with the slurries from water (PAA-H ₂ O) or DMF (PAA-DMF) and the composition was 80:10:10 (SiO _x : SP: PAA).....	6
Table S1. Discharge specific capacities of the SiO _x /PAA-DMF and SiO _x /PAA-H ₂ O electrodes at different current densities (1 C = 1500 mA·g ⁻¹).	7
Figure S4. The differential capacity plot of the SiO _x /PAA-H ₂ O (a) and SiO _x /PAA-DMF electrodes (b) Initial discharge/charge profiles of the SiO _x /PAA-H ₂ O and SiO _x /PAA-DMF electrodes under the current density of 0.1 C (c).....	8
Figure S5. Cycling performance (a) and rate capacity (b) of the Li SiO _x cells at 0.5 C in the voltage range of 0.01 V - 1.5 V with different volume ratios of H ₂ O/DMF with the mass loading density of 1.4-1.6 mg cm ⁻² with respect to SiO _x	9
Figure S6. Cycling performance of Li SiO _x cells at 0.5 C in the voltage range of 0.01 V - 1.5 V prepared with the slurries from NMP (PAA-NMP) or DMF (PAA-DMF) (the mass loading density of SiO _x is 1.4-1.6 mg cm ⁻²).....	10
Figure S7. Cycling performance of Li SiO _x cells at 0.5 C in the voltage range of 0.01 V - 1.5 V prepared with the slurries from the different molecular weights commercial aqueous PAA solutions or DMF/H ₂ O mixed PAA solutions: commercial aqueous PAA solution-1 (a) and commercial aqueous PAA solution-2 (b).	11
Figure S8. Cycling performance of Li SiO _x /C cells at 0.5 C in the voltage range of 0.01 V - 1.5 V prepared with the slurries from water (PAA-H ₂ O) or DMF (PAA-DMF) (1 C=450 mA g ⁻¹)	12
Figure S9. FTIR spectra of the PAA-H ₂ O and PAA-DMF solution (a). FTIR spectra of	

the SiO _x /PAA powder collected after drying treatment of the SiO _x -PAA-H ₂ O and SiO _x -PAA-DMF slurries (b). The shear rate dependent apparent viscosity evolution profiles of the PAA-H ₂ O and PAA-DMF solution with 10 wt% of PAA (c).	13
Figure S10. Top-view SEM images of the pristine SiO _x electrodes prepared with the PAA binder dissolved in the solvent mixture of DMF/H ₂ O with different volume ratios of H ₂ O/DMF.....	14
Figure S11. Digital photographs of pristine SiO _x electrodes with the PAA binder dissolved in the solvent mixture of H ₂ O/DMF with different volume ratios of H ₂ O/DMF.	15
Figure S12. Top-view SEM images of the pristine SiO _x /PAA-DMF (a, d, and g) and SiO _x /PAA-H ₂ O electrodes with the pH of 6 (b, e, and h) and 2 (c, f, and i).....	16
Figure S13. Digital photographs of the SiO _x /PAA-H ₂ O (a) and SiO _x /PAA-DMF electrodes (b) after 100 cycles.....	17
Figure S14. Digital photographs of SiO _x /PAA-DMF and SiO _x /PAA-H ₂ O electrodes after being folded once, twice, and three times, and their corresponding unfolded states (a-j).....	18
Figure S15. Cross-sectional SEM images of the SiO _x /PAA-H ₂ O electrode (a, b, c) and the SiO _x /PAA-DMF electrode (d, e, f) before cycling.....	19
Figure S16. The shear rate dependent apparent viscosity evolution profiles of the SiO _x -PAA-H ₂ O/DMF slurries and PAA-H ₂ O/DMF solution at similar viscosities.	20
Figure S17. Cycling performance of Li SiO _x cells at 0.5 C in the voltage range of 0.01 V - 1.5 V prepared with the slurries from water (PAA-H ₂ O) or DMF (PAA-DMF) at similar viscosities (a) and load-displacement curves of the SiO _x /PAA-H ₂ O and SiO _x /PAA-DMF electrodes prepared at this viscosity (b).	21
Table S2. The fractions of different peaks in XPS.....	22
Figure S18. Histogram of the resistivity of the SiO _x /PAA-DMF and SiO _x /PAA-H ₂ O electrodes.....	23
Figure S19. Calculation of isotactic, syndiotactic, and atactic PAA single point energies.	24

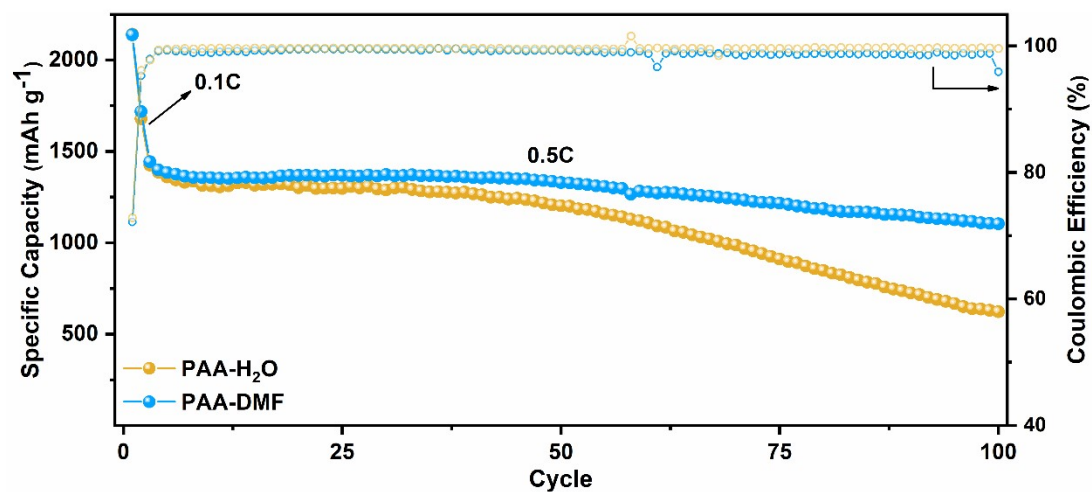


Figure S1. Cycling performance of Li||SiO_x cells at 0.5 C in the voltage range of 0.01 V - 1.5 V prepared with the slurries from water (PAA-H₂O) or DMF (PAA-DMF) with the mass loading density of SiO_x is 0.8 mg cm⁻².

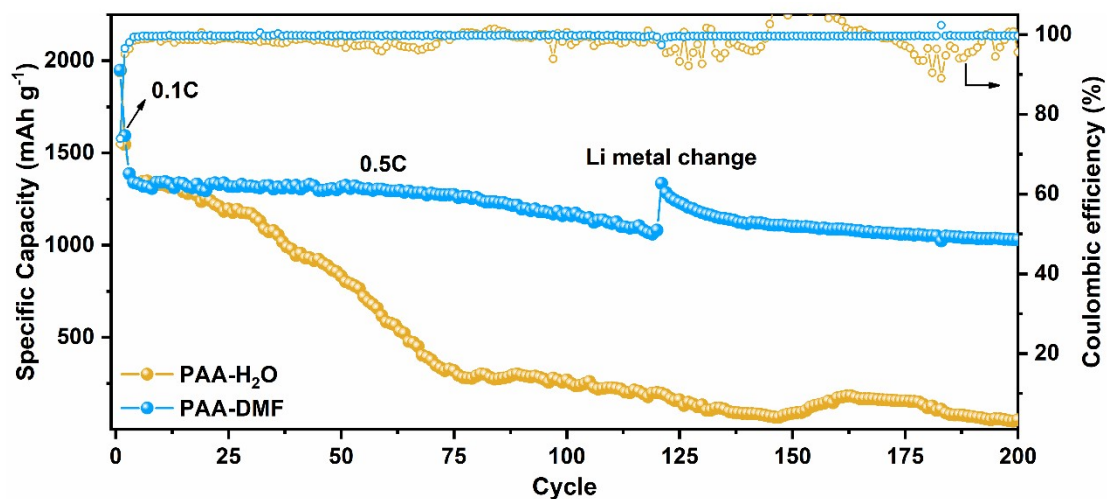


Figure S2. Cycling performance of Li||SiO_x cells at 0.5 C in the voltage range of 0.01 V - 1.5 V prepared with the slurries from water (PAA-H₂O) or DMF (PAA-DMF) with the lithium metal counter electrode is replaced after more than 100 cycles.

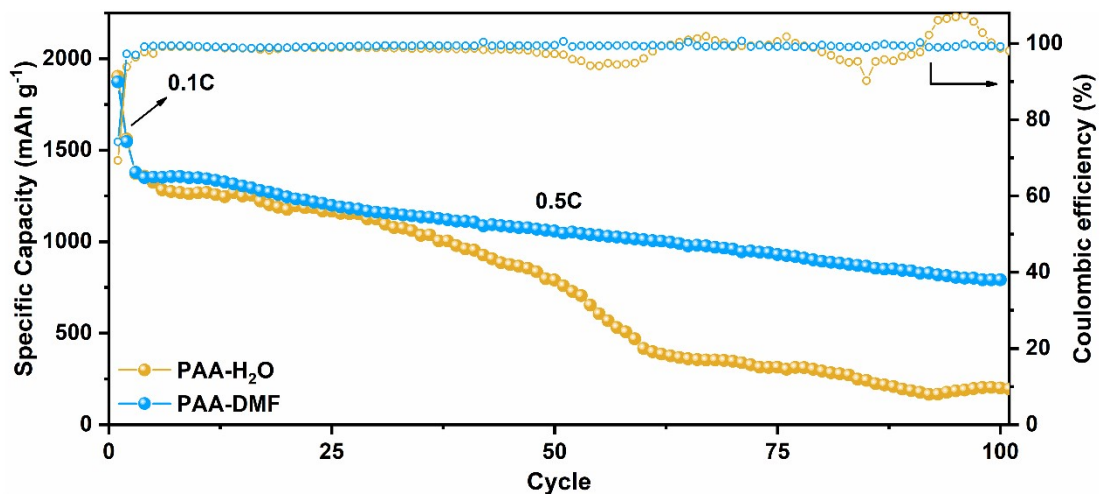


Figure S3. Cycling performance of Li||SiO_x cells at 0.5 C in the voltage range of 0.01 V - 1.5 V prepared with the slurries from water (PAA-H₂O) or DMF (PAA-DMF) and the composition was 80:10:10 (SiO_x: SP: PAA).

Table S1. Discharge specific capacities of the SiO_x/PAA-DMF and SiO_x/PAA-H₂O electrodes at different current densities (1 C = 1500 mA·g⁻¹).

Discharge Capacity (mAh·g ⁻¹)	Current densities					
	0.1 C	0.2 C	0.5 C	1 C	2C	0.2 C
SiO _x /PAA-DMF	1892	1618	1447	1094	648	1555
SiO _x /PAA-H ₂ O	1953	1506	1203	881	504	1329

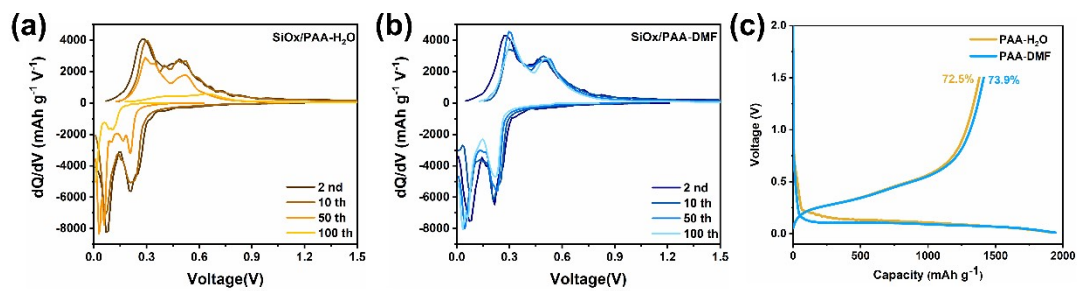


Figure S4. The differential capacity plot of the $\text{SiO}_x/\text{PAA-H}_2\text{O}$ (a) and $\text{SiO}_x/\text{PAA-DMF}$ electrodes (b) Initial discharge/charge profiles of the $\text{SiO}_x/\text{PAA-H}_2\text{O}$ and $\text{SiO}_x/\text{PAA-DMF}$ electrodes under the current density of 0.1 C (c).

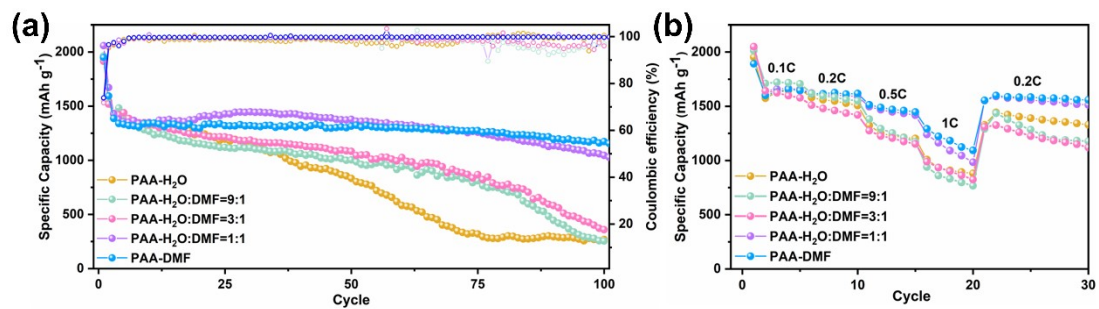


Figure S5. Cycling performance (a) and rate capacity (b) of the Li||SiO_x cells at 0.5 C in the voltage range of 0.01 V - 1.5 V with different volume ratios of H₂O/DMF with the mass loading density of 1.4-1.6 mg cm⁻² with respect to SiO_x.

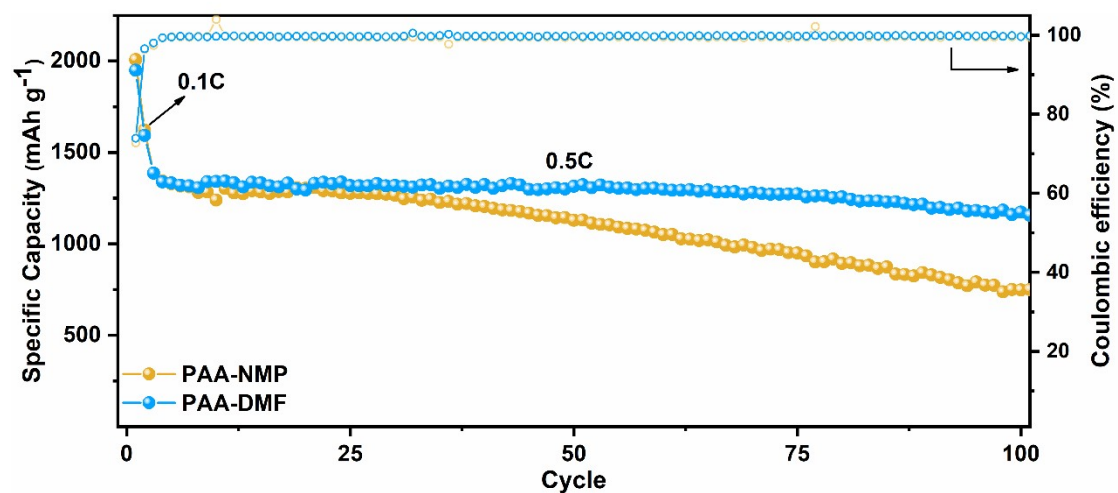


Figure S6. Cycling performance of Li||SiO_x cells at 0.5 C in the voltage range of 0.01 V - 1.5 V prepared with the slurries from NMP (PAA-NMP) or DMF (PAA-DMF) (the mass loading density of SiO_x is 1.4-1.6 mg cm⁻²).

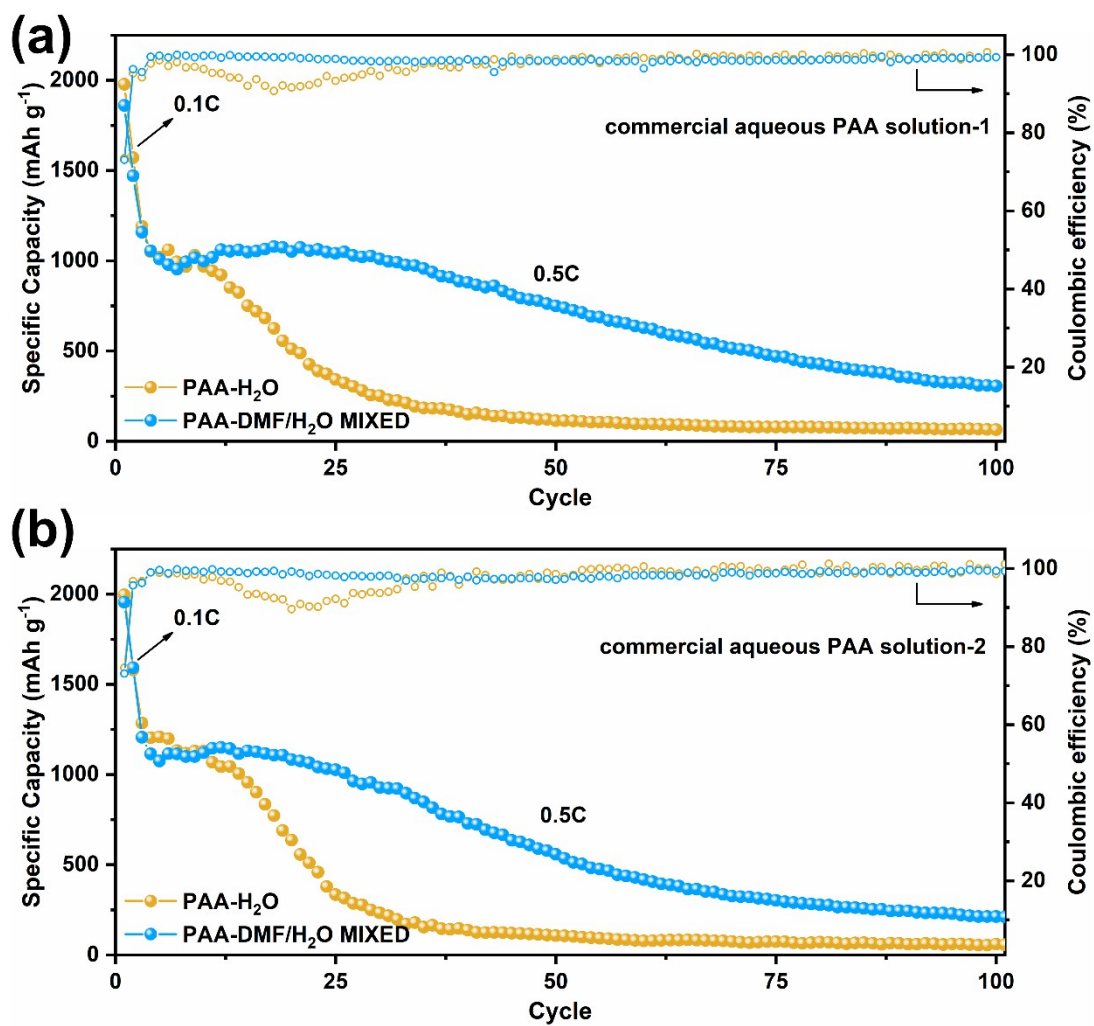


Figure S7. Cycling performance of Li||SiO_x cells at 0.5 C in the voltage range of 0.01 V - 1.5 V prepared with the slurries from the different molecular weights commercial aqueous PAA solutions or DMF/H₂O mixed PAA solutions: commercial aqueous PAA solution-1 (a) and commercial aqueous PAA solution-2 (b).

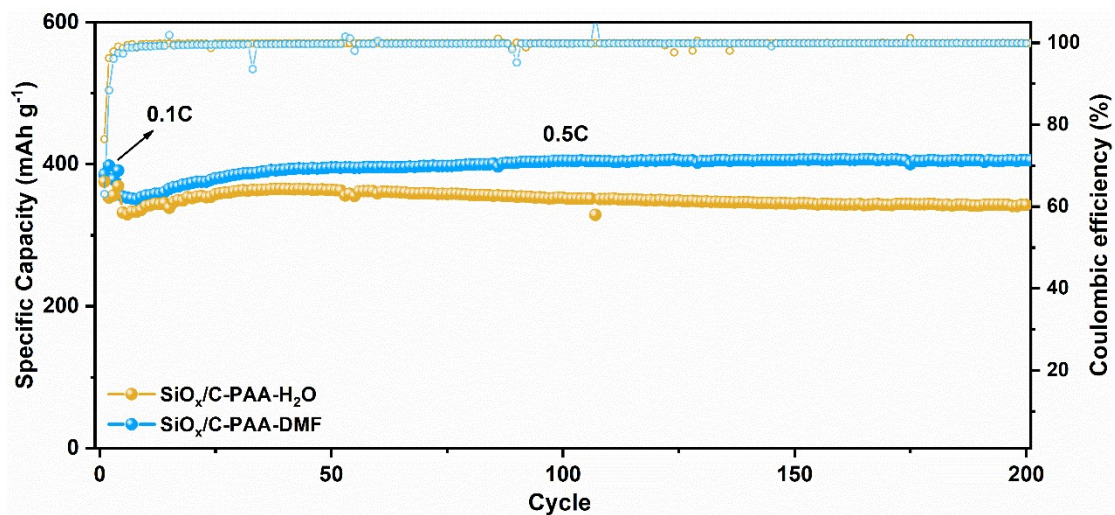


Figure S8. Cycling performance of Li||SiO_x/C cells at 0.5 C in the voltage range of 0.01 V - 1.5 V prepared with the slurries from water (PAA-H₂O) or DMF (PAA-DMF) (1 C=450 mA g⁻¹)

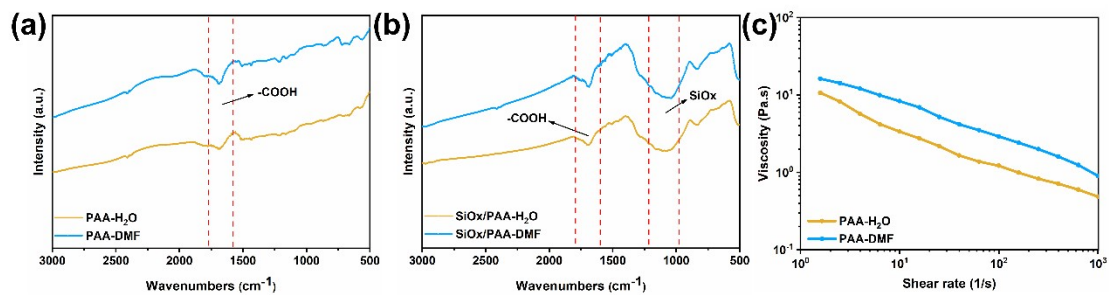


Figure S9. FTIR spectra of the PAA-H₂O and PAA-DMF solution (a). FTIR spectra of the SiO_x/PAA powder collected after drying treatment of the SiO_x-PAA-H₂O and SiO_x-PAA-DMF slurries (b). The shear rate dependent apparent viscosity evolution profiles of the PAA-H₂O and PAA-DMF solution with 10 wt% of PAA (c).

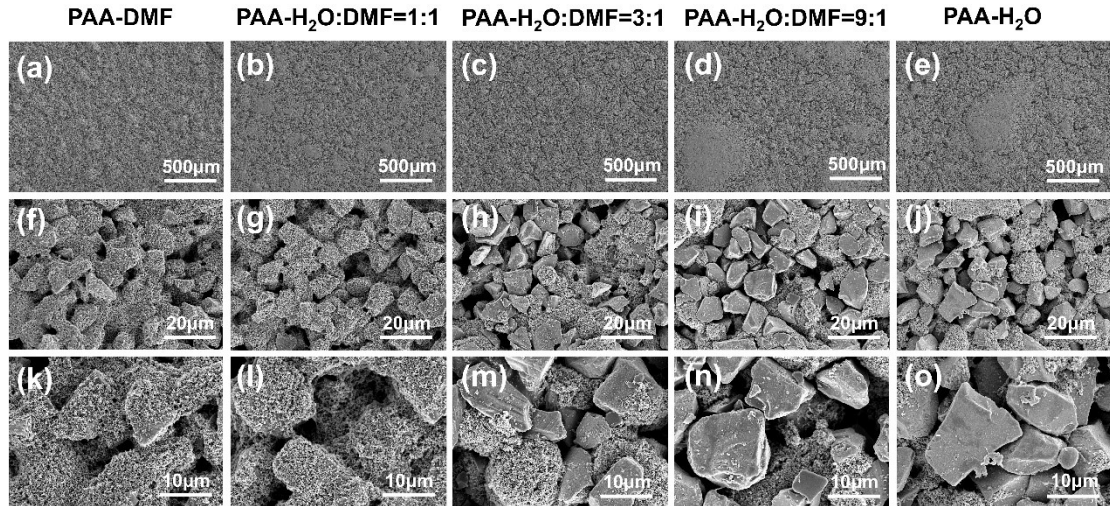


Figure S10. Top-view SEM images of the pristine SiO_x electrodes prepared with the PAA binder dissolved in the solvent mixture of DMF/H₂O with different volume ratios of H₂O/DMF.

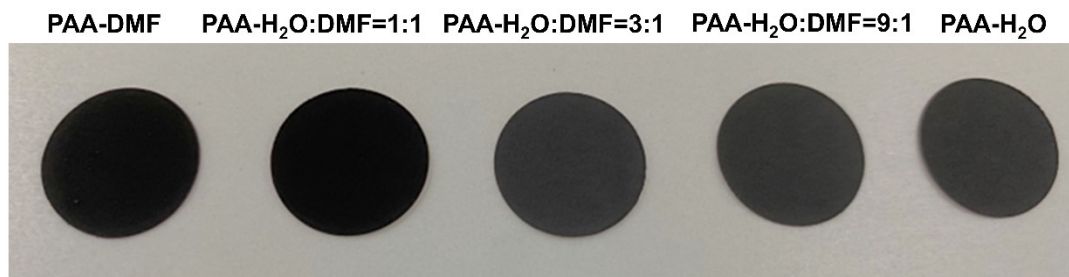


Figure S11. Digital photographs of pristine SiO_x electrodes with the PAA binder dissolved in the solvent mixture of H₂O/DMF with different volume ratios of H₂O/DMF.

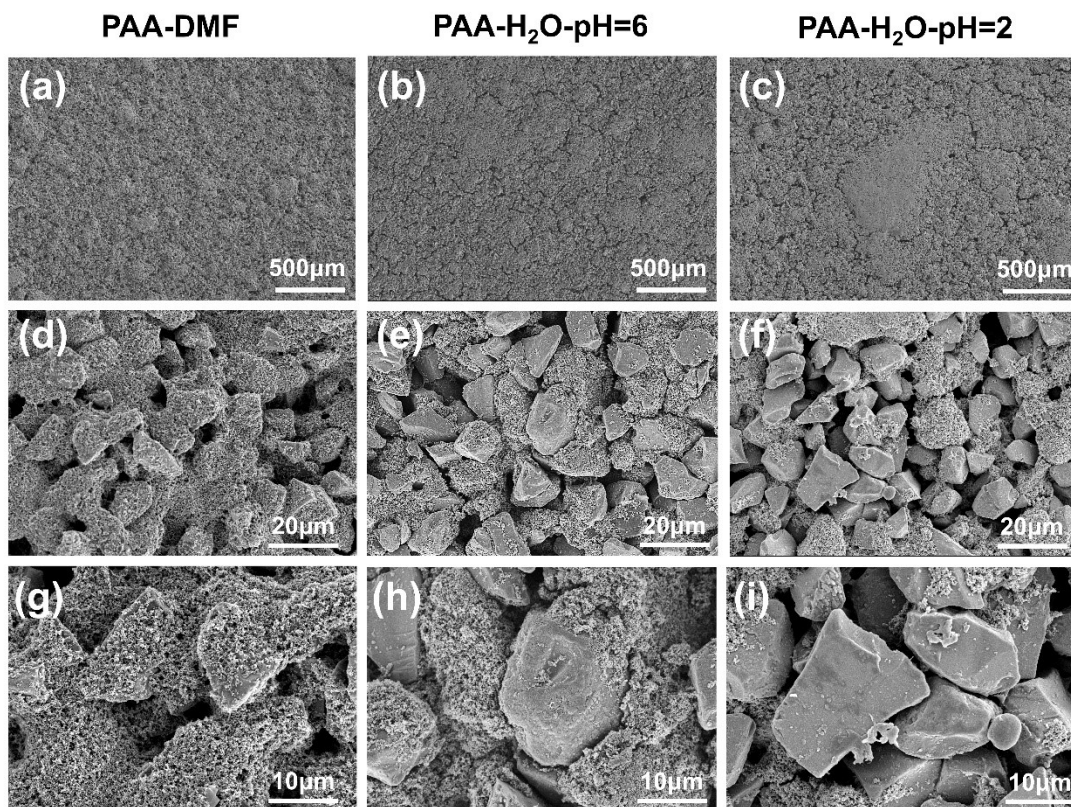


Figure S12. Top-view SEM images of the pristine SiO_x/PAA-DMF (a, d, and g) and SiO_x/PAA-H₂O electrodes with the pH of 6 (b, e, and h) and 2 (c, f, and i).

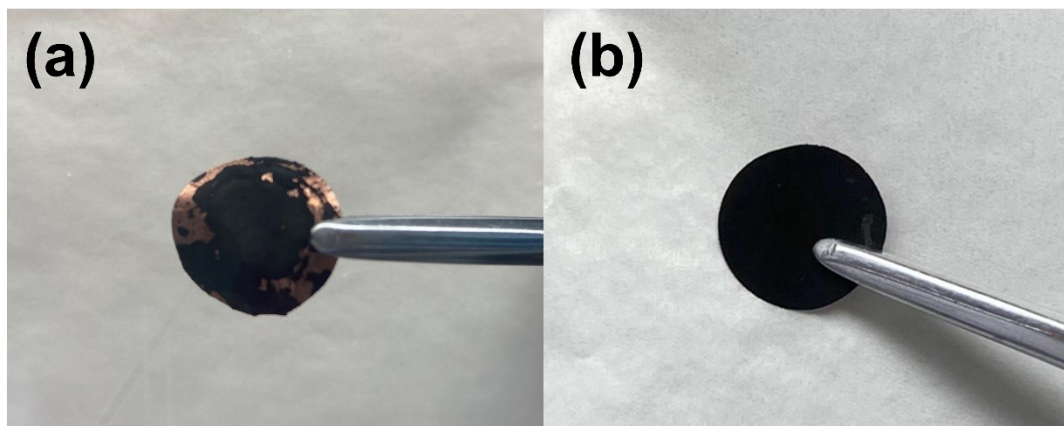


Figure S13. Digital photographs of the $\text{SiO}_x/\text{PAA-H}_2\text{O}$ (a) and $\text{SiO}_x/\text{PAA-DMF}$ electrodes (b) after 100 cycles.

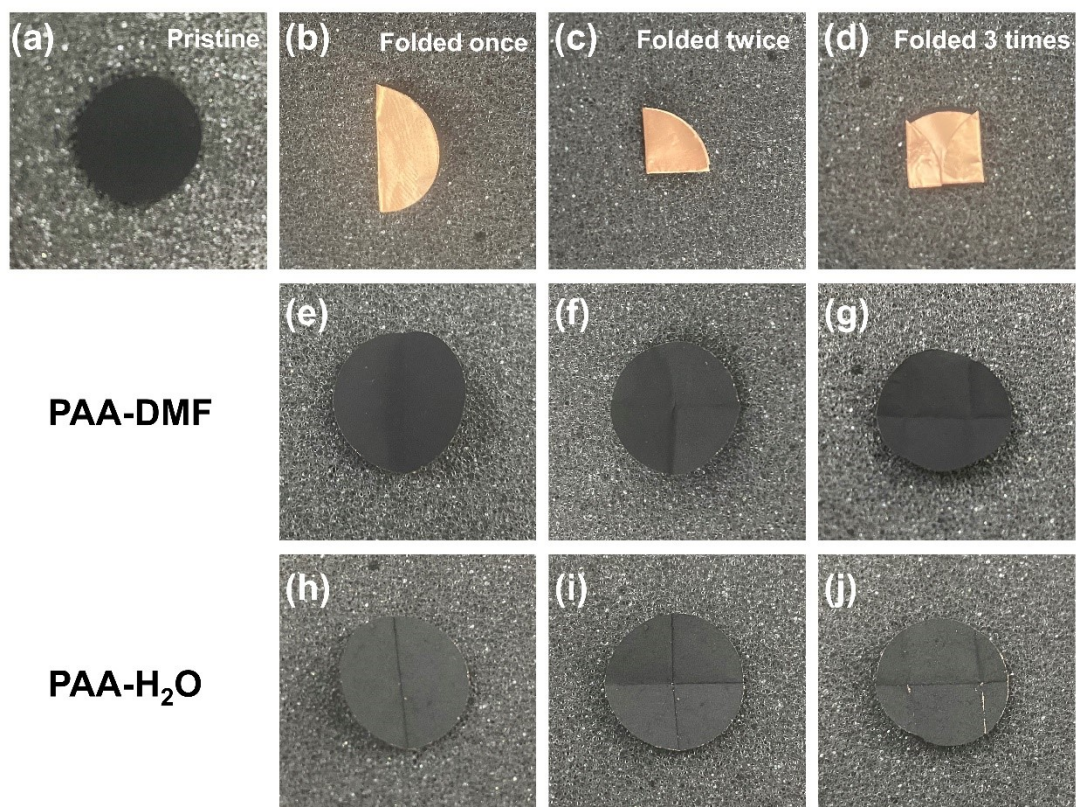


Figure S14. Digital photographs of SiO_x/PAA-DMF and SiO_x/PAA-H₂O electrodes after being folded once, twice, and three times, and their corresponding unfolded states (a-j).

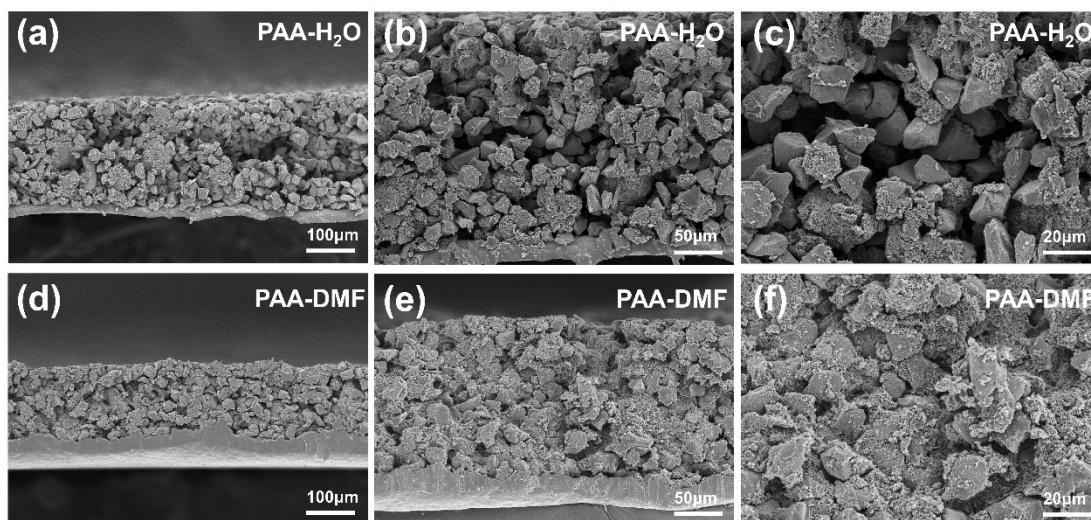


Figure S15. Cross-sectional SEM images of the SiO_x/PAA-H₂O electrode (a, b, c) and the SiO_x/PAA-DMF electrode (d, e, f) before cycling.

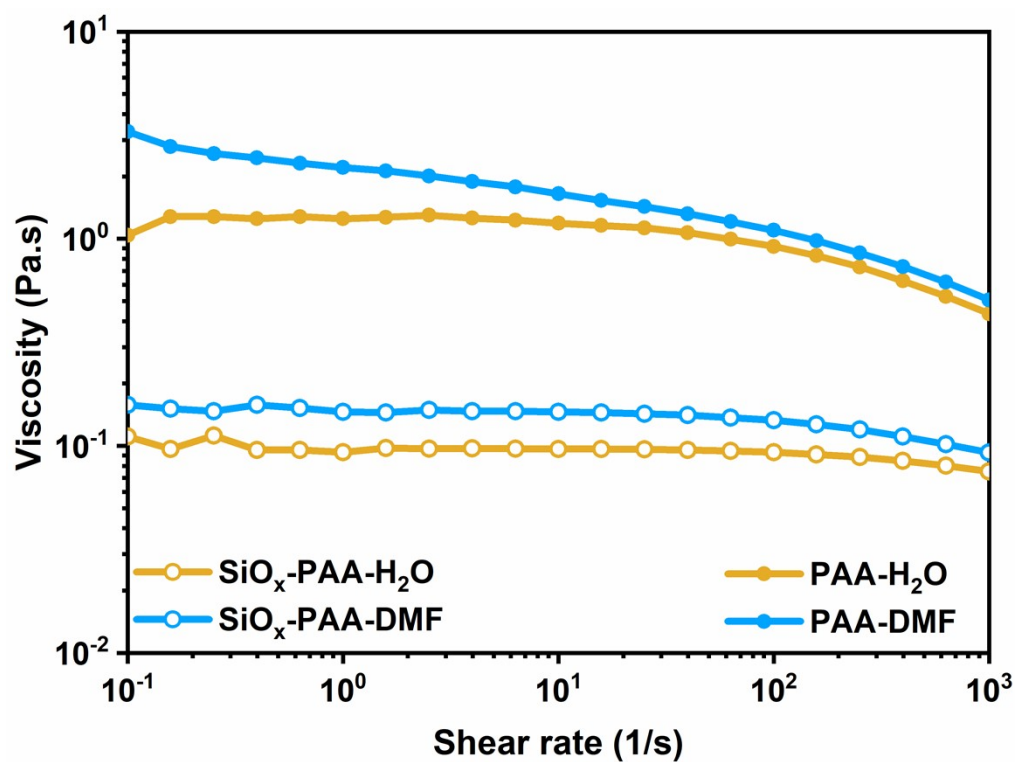


Figure S16. The shear rate dependent apparent viscosity evolution profiles of the SiO_x-PAA-H₂O/DMF slurries and PAA-H₂O/DMF solution at similar viscosities.

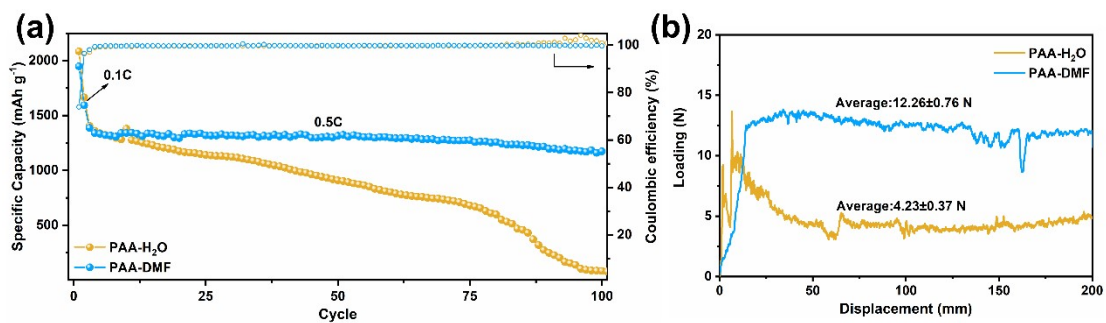


Figure S17. Cycling performance of Li||SiO_x cells at 0.5 C in the voltage range of 0.01 V - 1.5 V prepared with the slurries from water (PAA-H₂O) or DMF (PAA-DMF) at similar viscosities (a) and load-displacement curves of the SiO_x/PAA-H₂O and SiO_x/PAA-DMF electrodes prepared at this viscosity (b).

Table S2. The fractions of different peaks in XPS.

%	C 1s				O 1s			F 1s	
	C-C/ C-H	C-O	C=O	Li ₂ CO ₃	C-O	Li ₂ CO ₃	Li ₂ O	Li _x PF _y	LiF
SiO_x/PAA -DMF	50.51	32.17	7.06	10.26	27.34	67.94	4.72	79.42	20.58
SiO_x/PAA -H₂O	44.16	19.75	6.45	29.64	43.22	55.25	1.53	89.03	10.97

The data for the different peak fractions shows that the SiO_x/PAA-DMF electrode produces less Li₂CO₃ and more LiF than the SiO_x/PAA-H₂O electrode. The SiO_x/PAA-DMF electrode forms a stable SEI layer, which helps to inhibit electrolyte decomposition, and the LiF-rich SEI layer also has a higher shear modulus, which better inhibits volume expansion during cycling.

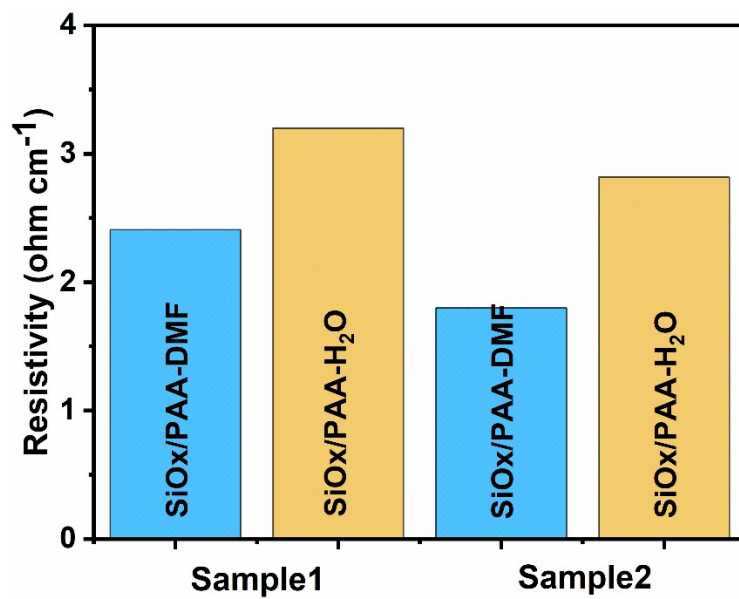


Figure S18. Histogram of the resistivity of the SiO_x/PAA-DMF and SiO_x/PAA-H₂O electrodes.

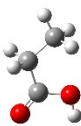
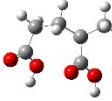
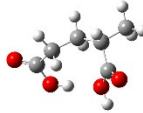
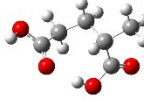
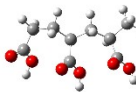
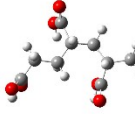
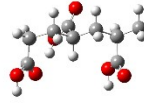
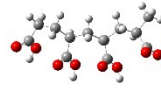
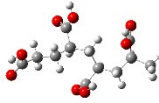
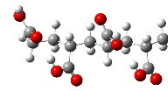
DP	Isotactic(eV)	Syndiotactic (eV)	Atactic (eV)
1	 -7305.64	/	/
2	 -14571.61	 -14571.47	 -14571.55
3	 -21851.64	 -21851.61	 -21851.62
4	 -29124.50	 -29123.95	 -29124.22

Figure S19. Calculation of isotactic, syndiotactic, and atactic PAA single point energies.

The results for the single point energies of isotactic, syndiotactic, and atactic PAA show that the energies of the three are close to each other, with the isotactic PAA having lower single point energies at different degrees of polymerization, the atactic PAA being in the middle and the syndiotactic being the highest. In this paper, the lower energy isotactic PAA was chosen for the calculation of the subsequent solvent molecular binding energy.